Chemical Geology xxx (xxxx) xxx–xxx

Contents lists available at ScienceDirect

Chemical Geology

journal homepage: www.elsevier.com/locate/chemgeo

Groundwater geochemistry fluctuations along a fresh-saltwater gradient on the carbonate islands of the lower Florida Keys

Danielle E. Ogurcak[a,*], René M. Price[a,b]

[a] Department of Earth and Environment, Florida International University, 11200 SW 8th Street, Miami, FL 33199, USA
[b] Southeast Environmental Research Center, Florida International University, 11200 SW 8th Street, Miami, FL 33199, USA

ARTICLE INFO

Keywords:
Carbonate islands
Climate change
Florida Keys
Freshwater lens
Salinity gradient

ABSTRACT

Climate change will have long-lasting effects on the availability of fresh water on small, carbonate islands that have isolated fresh groundwater lenses, particularly as sea level rises and rainfall regimes shift. The carbonate islands of the Florida Keys provide an ideal location to study the effect of variable rainfall on the aqueous geochemistry of the islands' groundwater. In a rainfall-driven carbonate system, the expectation is that limestone dissolution will occur within the vadose zone resulting in increased ions in the groundwater. However, geochemical processes are also affected by the salinity of groundwater and the extent of the mixing zone between fresh and salt water. We chose two islands to conduct the study of the shallow groundwater: the largest island in the lower Florida Keys, Big Pine Key (BPK), and a smaller island, Upper Sugarloaf Key (SLK). From May 2011 through April 2012, monthly groundwater samples were collected from 24 shallow (1 m deep) wells located along a fresh to saline gradient on both islands. Groundwater chemistry was compared with rainfall amounts from a weather station on BPK. Saturation indices for aragonite and calcite, generated with geochemical modeling in PHREEQC, were compared to conservative mixing between Gulf of Mexico water and freshwater. Equilibrium to supersaturated conditions with respect to carbonate minerals dominated in all of the groundwater samples. Saturation indices varied with rainfall with the most supersaturated samples observed after a large rain event and samples approaching equilibrium after the longest period without rainfall. Calcium in excess of what would be expected from conservative mixing of fresh water and seawater was observed in all groundwater samples and was elevated at near-shore locations, especially on BPK. Contrary to expectations, dissolution resulting from mixing of freshwater and seawater was not supported in the shallow groundwater. Instead, dissolution within the narrow vadose zone from rain events likely resulted in the excess calcium in the groundwater. Seasonal fluctuations in groundwater composition were primarily observed on the smaller island and were related to the fresh water balance, changing rapidly after a heavy rain event, and suggest that a size threshold has been surpassed for a stable lens. Rising seas will further decrease lens extent and vadose zone depth, reducing the potential for future limestone dissolution.

1. Introduction

Small oceanic islands that are threatened by sea level rise and associated salt water intrusion will also be subject to variable precipitation and evapotranspiration (ET) in the next century resulting from global climate change (Wong et al., 2014). Changes to geochemical reactions within the mixing zone between fresh and salt water can either enhance or degrade storage capacity of the surficial aquifer in karst systems. In the Florida Keys, carbonate islands support a variety of endemic plants and animals that rely on a shallow freshwater lens recharged by rainfall (Ross et al., 1994). Rainfall predominantly occurs in a summer wet season in south Florida followed by several months of drought; however the timing of the rainfall can shift to the winter season during ENSO events (Childers et al., 2006). Current climate change scenarios for south Florida suggest a modest change in rainfall (+/− 10%), but when combined with a 1.5% increase in temperature and a 0.46 m increase in sea level the impact on freshwater resources can be significant (Obeysekera et al., 2015).

The geochemistry of groundwater on carbonate islands is driven by interactions of rainfall and seawater within the carbonate aquifer

Abbreviations: BPK, Big Pine Key; ENSO, El Nino Southern Oscillation; DTC, Distance to coast; GMWL, Global Meteoric Water Line; PET, potential evapotranspiration; SLK, Upper Sugarloaf Key; TBK, Tarpon Belly Keys

* Corresponding author at: Institute of Water & Environment, Florida International University, 11200 SW 8th Street, Miami, FL 33199, USA.
E-mail address: dogurcak@fiu.edu (D.E. Ogurcak).

https://doi.org/10.1016/j.chemgeo.2018.09.032
Received 4 November 2017; Received in revised form 24 July 2018; Accepted 22 September 2018

(Anthony et al., 1989). In a rainfall-driven carbonate system, the expectation is that dissolution will occur within the vadose zone resulting in increased ions in the groundwater until saturation with respect to the carbonate minerals (Langmuir, 1997). However, geochemical processes are also affected by the salinity of groundwater and the extent of the mixing zone between fresh and salt water (Back and Hanshaw, 1970). For instance, ion exchange process and carbonate mineral dissolution have been documented as seawater intrudes into coastal carbonate aquifers (Price et al., 2010; Flower et al., 2017). Periodic flooding of the islands with seawater during extreme high tides or storm surges, followed by evaporation with little to no rain, can lead to hypersaline conditions and the formation of evaporite minerals (Swart and Kramer, 1997).

The Florida Keys provided an ideal location to study the combined effects of variable rainfall, evapotranspiration (ET) and saltwater intrusion on the aqueous geochemistry of groundwater on carbonate islands. We chose two islands to conduct the study: the largest island in the lower Florida Keys, Big Pine Key (BPK), and a smaller island, Upper Sugarloaf Key (SLK). We investigated changes in rock-water interactions across a gradient of fresh to brackish groundwater throughout a year of unusual rainfall. The overall purpose of the investigation was to determine how geochemical conditions in the shallow groundwater change under varying conditions of saltwater intrusion, rainfall, and ET. The objectives of this investigation were two-fold: 1) to determine how geochemical conditions in the groundwater vary across a salinity gradient on lenses of variable size, and 2) to determine how the groundwater geochemistry changes with varying rainfall and ET. The results of this investigation can lead to insights on the effects of anthropogenic climate change on groundwater resources in carbonate islands.

2. Materials and methods

2.1. Study area

The islands of Big Pine Key (N 24.67, W 81.36) and Upper Sugarloaf Key (N 24.66, W 81.53) are located toward the distal end of the chain of islands known as the Florida Keys (Fig. 1). The climate is humid subtropical, becoming increasingly warm and dry as one moves south through the chain of islands. Precipitation is seasonal with a distinct wet season (June through October) in which approximately two-thirds of the rain in any given year falls, followed by a dry season (November through May) (Duever et al., 1994). The annual average rainfall is 102.2 cm and temperatures range from an average monthly low of 20 °C to a high of 29 °C, in January and August, respectively (30-year average 1984–2013 at Key West International Airport, http://www.ncdc.noaa.gov). Rainfall events can be sporadic, with large quantities of precipitation accompanying tropical storms. For south Florida, the average tropical storm/hurricane return interval is 3 years, with Cat 3–5 storms occurring at an interval of every 15 years for Key West (Keim et al., 2007).

The surficial bedrock of the Florida Keys was deposited in the late Pleistocene during the last interglacial period and has been dated to 134,000 years BP (Perkins, 1977). The exposed bedrock formation in the upper and middle keys is Key Largo Limestone, derived from a shallow water shelf margin coral reef (Harrison and Coniglio, 1985) of peloid-bioclast packstone-grainstone (Hoffmeister and Multer, 1968). In the lower Keys, the surficial bedrock is the Miami Limestone, which was formed in a backbay environment as a former tidal sandbar (Hoffmeister et al., 1967) and consists of ooid grainstone. Beginning on Big Pine Key and trending to the southwest, the Miami Limestone crops out over the underlying Key Largo Limestone and contacts are separated by subaerial exposures (Coniglio and Harrison, 1983). Both formations are moderately to highly porous (average porosity of 20 to 40%) (Robinson, 1967; DiFrenna et al., 2008), but the Key Largo Limestone is more permeable than the Miami Limestone as a result of the greater development of secondary porosity (Coniglio and Harrison, 1983). The greater permeability and thus hydraulic conductivity of the Key Largo Limestone, 1400 m/d compared with 120 m/d in the Miami Limestone (Vacher et al., 1992), results in the freshwater lens on the islands being truncated at the contact between the formations. This occurs at an approximate depth of 5 m below the ground surface (Hanson, 1980). For Big Pine Key, time needed for rainfall infiltrating at the center of the island to travel through the aquifer to the coast is 8 years (Wightman, 1990).

Twentieth century residential development on both islands has certainly affected aquifer recharge and discharge and canal dredging has been estimated to have resulted in a 20% loss of the lens volume on BPK compared to pre-development conditions (Langevin et al., 1998). While some residents do extract water from the lenses for outdoor residential use, this is likely a negligible output from the system. Additional inputs to the system occur from septic seepage as potable water is provided via the Florida Aqueduct Authority to residential homes and businesses from the Biscayne Aquifer on the Florida mainland. However, many of these homes are associated with the network of canals and the additional source of water very likely flows to the adjacent Florida Bay or Atlantic Ocean. In the relatively undeveloped portions of the islands where we conducted our research, these additional inputs and outputs should have minimal impact, and instead the difference in size between the islands should drive extent of the freshwater lenses on each.

2.2. Climate data

Weather data were obtained from a station (TS607) operated by the National Key Deer Refuge and located at the north end of BPK (N 24.72422, W 81.38864). Hourly rainfall, temperature, and solar radiation data, for April 2011 through March 2012, were downloaded from MesoWest (website maintained by the University of Utah, http://mesowest.utah.edu/cgi-bin/droman/mesomap.cgi?state=FL&rawsflag=3). Data recorded by the station were used to generate monthly totals for precipitation (mm) and potential evapotranspiration (PET) (mm). The weather station was equipped with a pyranometer placed at a height of 2 m above the ground surface to record solar radiation and a tipping bucket rain gauge to record the amount of rainfall. The Simple Abtew method (Abtew, 1996) was used to estimate daily potential evapotranspiration (PET) with the following equation:

$$PET = K_1 * R_s / \lambda \quad (1)$$

where PET is potential evapotranspiration in mm/day, K_1 is a dimensionless coefficient equal to 0.53, R_s is solar radiation as measured in MJ/m^2/day, and λ is equal to the latent heat of vaporization of water with units of MJ/kg and varies with temperature according to the following equation:

$$\lambda = 2.501 - 0.00263 * T \quad (2)$$

where T is equal to daily average temperature in ° Celsius. Results obtained from this method for Everglades' wetlands are comparable to other methods of PET estimation requiring a greater number of parameters (Abtew, 1996). Monthly rainfall accumulation was compared to the 30-year average (1983–2012) for each month from the station at Key West International Airport, data available from the National Climate Data Center (http://www.ncdc.noaa.gov/).

2.3. Isotopic data

Rainfall collectors were also established on both islands to collect rainfall samples for isotopic composition of oxygen and hydrogen. The collectors consisted of 2-L reservoir glass bottles, equipped at the top with a 7.5 cm diameter funnel secured into a silicone stopper that was vented with a small diameter needle. A 1 cm layer of mineral oil was placed in each bottle to prevent evaporation (Scholl et al., 1996).

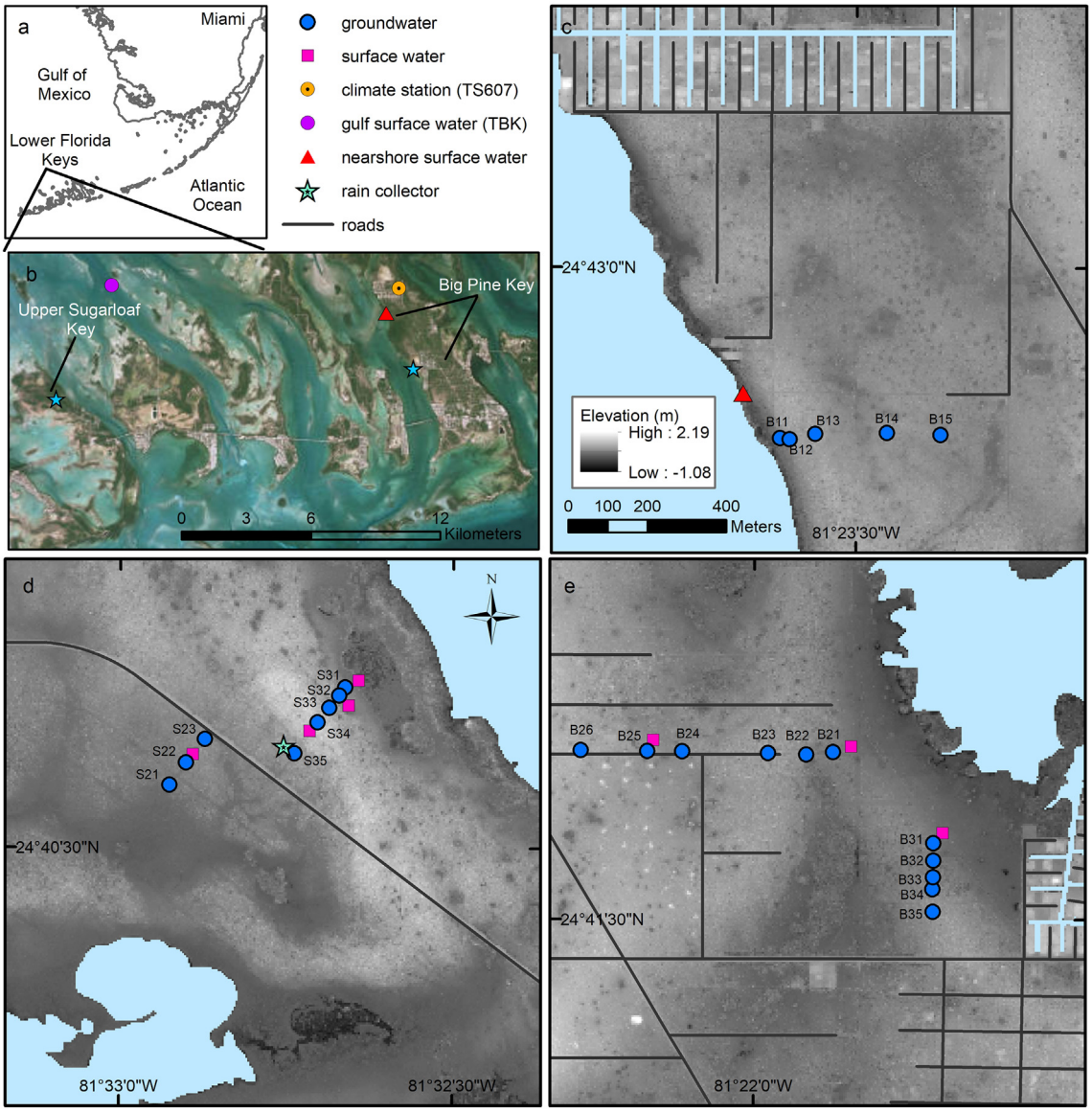

Fig. 1. Study sites on Big Pine (BPK) and Upper Sugarloaf Keys (SLK) in the lower Florida Keys. The regional map indicates the location of the lower Florida Keys in relation to mainland Florida (a). The aerial map of the lower Florida Keys (b) shows the location of the climate station (TS607), rain collectors, and gulf (TBK) and nearshore surface water sampling. Scale and elevation ramp apply to maps (c, d, and e) which indicate the location of groundwater monitoring wells and nearby surface water collection sites relative to the coast.

Collectors had an outlet valve at their base to obtain a sample that minimized the amount of oil included in the sample for subsequent isotopic analysis. Water samples were collected monthly, and the total monthly volume of precipitation accumulated in each bottle was recorded. The rain collectors were placed in open areas free of overhanging branches or obstructions. The collector on BPK was located on the grass outside of the refuge headquarters building. The collector on SLK was located on open rock in a clearing along the northern transect. Both collectors were placed on low concrete platforms approximately 5 cm off the ground and were housed inside a wooden box in which only the funnel opening was visible at the top to the outside. The structure provided both a stable platform and shade to further minimize potential evaporation. The weighted mean $\delta^{18}O$ and $\delta\ ^{2}H$ (WMδ) of the collected rainfall monthly at each collector for the sampling period of March 2011 through March 2012 (n = 12; one month missing from each collector) was calculated using the following equation:

$$WM\delta = \sum_{i=1}^{n} \left(\delta_{smpl} * \frac{V_{smpl}}{V_{study}} \right) \quad (3)$$

where δ_{smpl} is equal to the value of the isotope measured in a collector for a particular month, V_{smpl} is the volume of rainfall accumulated in the same month, and V_{study} is the volume of rainfall accumulated over the entire study period for that collector.

2.4. Groundwater and surface water geochemistry

Beginning in May 2011 and ending in April 2012, groundwater and surface water were collected on a monthly basis in shallow monitoring wells, nearby karst depressions, and in a tidally-influenced mangrove fringe forest, and analyzed for major cations, anions, and alkalinity. At quarterly intervals, samples were also collected for oxygen and hydrogen isotopic analysis. Wells were installed across a gradient of forest community types and coastal proximity along five transects coincident with trails or unpaved roads located within the U.S. Fish & Wildlife Service (USFWS) National Key Deer Refuge and an uninhabited

Table 1
Means +/− SE are reported for depth to water table (m), salinity (ppt), calcite and aragonite saturation indices (SIs), and $\delta^{18}O$ measured monthly or quarterly at each groundwater monitoring well throughout the study (May 2011 to April 2012). The value for April 2012 SIs are not included due to miscalibrated pH probe. Elevation is the average of pixels from Lidar DTM contained within a 5 m radius circle inscribing each well or surface water location and distance to coast (DTC) is calculated as nearest straight-line distance to coastline. Number of months sampled for surface water (sw) sites B25, B31, S23, and S34 was limited by available standing water (n = 8, 9, or 10).

Well/surface water	Elev (m)	DTC (m)	Depth to H_2O table (m) (n = 12)	Salinity (ppt) (n = 12)	Calcite SI (n = 11)	Aragonite SI (n = 11)	$\delta^{18}O$ (n = 4)
B11	0.18	37	0.31 ± 0.03	6.68 ± 0.09	0.40 ± 0.05	0.26 ± 0.04	−2.50 ± 0.04
B12	0.51	53	0.58 ± 0.03	2.63 ± 0.16	0.48 ± 0.05	0.33 ± 0.05	−3.01 ± 0.08
B13	0.75	113	0.71 ± 0.03	1.46 ± 0.05	0.41 ± 0.06	0.26 ± 0.06	−3.00 ± 0.04
B14	0.51	277	0.47 ± 0.03	0.73 ± 0.04	0.36 ± 0.06	0.22 ± 0.06	−3.71 ± 0.43
B15	0.41	401	0.35 ± 0.03	0.49 ± 0.02	0.39 ± 0.06	0.24 ± 0.06	−2.98 ± 0.30
B21	0.26	191	0.39 ± 0.04	19.45 ± 1.79	0.53 ± 0.06	0.39 ± 0.06	−1.80 ± 0.37
B22	0.30	249	0.50 ± 0.03	8.14 ± 0.14	0.46 ± 0.06	0.32 ± 0.06	−3.07 ± 0.08
B23	0.62	332	0.48 ± 0.03	1.64 ± 0.06	0.45 ± 0.07	0.31 ± 0.07	−2.32 ± 0.09
B24	0.46	532	0.44 ± 0.03	0.74 ± 0.08	0.32 ± 0.05	0.18 ± 0.05	−2.86 ± 0.45
B25	0.60	621	0.64 ± 0.03	2.56 ± 0.12	0.58 ± 0.08	0.43 ± 0.08	−2.82 ± 0.08
B26	0.88	682	0.76 ± 0.03	0.43 ± 0.02	0.38 ± 0.05	0.24 ± 0.05	−3.67 ± 0.09
B31	0.22	150	0.34 ± 0.03	14.27 ± 0.17	0.60 ± 0.06	0.46 ± 0.06	−0.69 ± 0.04
B32	0.37	188	0.31 ± 0.03	13.02 ± 0.39	0.51 ± 0.05	0.37 ± 0.05	−1.03 ± 0.03
B33	0.32	227	0.53 ± 0.03	6.03 ± 0.16	0.38 ± 0.05	0.24 ± 0.05	−2.71 ± 0.16
B34	0.49	254	0.52 ± 0.03	2.93 ± 0.25	0.31 ± 0.05	0.17 ± 0.05	−3.48 ± 0.32
B35	0.55	300	0.50 ± 0.03	3.08 ± 0.02	0.42 ± 0.06	0.28 ± 0.06	−3.05 ± 0.06
S21	0.05	394	0.14 ± 0.03	20.27 ± 1.09	0.51 ± 0.07	0.37 ± 0.07	−0.90 ± 0.20
S22	0.37	456	0.28 ± 0.04	5.63 ± 0.19	0.42 ± 0.07	0.28 ± 0.07	−2.57 ± 0.16
S23	0.42	525	0.29 ± 0.04	2.43 ± 0.03	0.43 ± 0.08	0.29 ± 0.08	−2.17 ± 0.09
S31	0.33	239	0.33 ± 0.04	28.40 ± 1.50	0.43 ± 0.06	0.29 ± 0.06	−0.50 ± 0.45
S32	0.58	261	0.44 ± 0.04	7.68 ± 0.96	0.34 ± 0.07	0.20 ± 0.07	−3.41 ± 0.60
S33	0.70	295	0.57 ± 0.03	2.38 ± 0.30	0.45 ± 0.06	0.31 ± 0.06	−3.44 ± 0.37
S34	1.14	338	0.91 ± 0.04	1.02 ± 0.14	0.32 ± 0.05	0.18 ± 0.05	−4.23 ± 0.50
S35	0.59	405	0.40 ± 0.04	0.95 ± 0.08	0.42 ± 0.06	0.28 ± 0.06	−2.81 ± 0.27
B21sw	0.15	144	na	31.66 ± 3.68	1.36 ± 0.05	1.22 ± 0.05	na
B25sw	−0.01	601	na	0.83 ± 0.10	1.27 ± 0.09	1.13 ± 0.09	1.10 ± 0.40
B31sw	0.12	117	na	48.36 ± 6.01	1.19 ± 0.07	1.05 ± 0.07	na
S23sw	0.40	479	na	3.64 ± 0.27	0.86 ± 0.11	0.72 ± 0.11	na
S31sw	0.04	205	na	37.84 ± 1.07	0.87 ± 0.08	0.73 ± 0.08	na
S32sw	−0.09	245	na	45.31 ± 4.30	1.05 ± 0.07	0.90 ± 0.07	na
S34sw	0.33	357	na	2.04 ± 0.25	1.10 ± 0.11	0.96 ± 0.11	na

inholding on BPK and SLK for a total of 24 wells (Fig. 1). Wells were named with an alpha-numeric code that includes the first letter of each island name, the transect number for each island, and the well position along each transect in relation to the coast (Table 1). Boreholes with diameters of 8.89 cm were drilled through bedrock to a depth of 1 to 1.25 m below the ground surface. Within each borehole was placed a PVC pipe with an internal diameter of 3.175 cm, screened along the bottom 0.5 m so that groundwater entered the well at a depth of 0.5 to 1.25 m below the ground surface. Wells were packed with sand to a level above the well screen and finished with cement. GPS coordinates were obtained for each well using a Magellan ProMark™ 3 system having a horizontal accuracy of 10 cm. Elevation in NAVD88 was obtained for each well and surface sampling location from a digital elevation model (DEM) derived from LiDAR having a spatial resolution of 5 m^2 (Zhang et al., 2010). Coastal proximity was defined as the distance to the nearest shoreline.

Prior to each sampling event, the depth (cm) to the water table was recorded and three well volumes were then evacuated with a peristaltic pump. Conductivity, temperature, and pH were measured in situ, the first two using a YSI Model 30™ handheld probe (Yellow Springs, OH) and the latter with an Orion Three-Star™ pH meter (Thermo Scientific, Beverly, MA). The relative accuracy of each field parameter was ± 0.1 °C, ± 0.1 mS/cm, and ± 0.002, respectively. Groundwater was collected and filtered using a 0.45 µm membrane filter into four 60 mL bottles, one of which was preserved with 10% hydrochloric acid for cation analysis. Surface water samples were collected unfiltered. All sample bottles were immediately closed, placed on ice and transported back to Florida International University to be stored at 4 °C. Unfiltered samples were filtered in the lab with a 0.45 µm membrane filter prior to analysis. Alkalinity titrations were conducted within 24 h of sample collection on filtered water samples using a Brinkman Titrino 751 Titrator with 0.1 M concentration of HCl to a pH of 2. Total alkalinity was determined by the amount of acid added at the lowest inflection point of the titration curve, and reported in units of milliequivalents per liter (meq/L) of bicarbonate [$HCO3^-$]. Concentrations of both major cations and anions, including calcium [Ca^{2+}], magnesium [Mg^{2+}], sodium [Na^+], potassium [K^+], chloride [Cl^-], and sulfate [SO_4^{2-}] were analyzed using a Dionex-120 Ion Chromatograph. A charge balance was calculated for major cations and anions, including HCO_3^-, for each sample, of 377 groundwater and surface water samples, only 12 had charge balance errors > 5% (but still < 8%).

A sea surface sample was obtained from the Gulf of Mexico near Tarpon Belly Keys (TBK) (N 24.72503, W 81.52052) as part of the Southeast Environmental Research Center (SERC) Water Quality Monitoring Project quarterly sampling events (http://serc.fiu.edu/wqmnetwork/FKNMS-CD/index.htm) (Fig. 1). Four sampling dates spanned the year of groundwater sampling and included collections on April 26, 2011, July 25, 2011, December 7, 2011, and February 8, 2012. Samples were transported to FIU and stored at 4 °C. Samples were analyzed for cations and anions, following the above procedure for groundwater and surface water. Alkalinity was calculated from an equation relating sea surface salinity (SSS) and sea surface temperature (SST) to surface total alkalinity (A_T) for oceans of the subtropics (30°S to 30°N) (Lee et al., 2006):

$$A_T = 2305 + 58.66\,(SSS - 35) + 2.32\,(SSS - 35)^2 - 1.41\,(SST - 20) + 0.040\,(SST - 20)^2 \quad (4)$$

Monthly precipitation chemistry data were obtained from the National Atmospheric Deposition Program (NADP) National Trends

Network (NTN) site located in Everglades National Park (NTN Site FL11; http://nadp.slh.wisc.edu/data/sites/siteDetails.aspx?net=NTN&id=FL11) for the period of groundwater sampling. Alkalinity as [HCO3$^-$] was calculated from the following equation (Kulshrestha et al., 2003):

$$[HCO_3^-] = 10^{(pH-5.05)} \quad (5)$$

2.5. PHREEQC modeling

Calcite and aragonite ($CaCO_3$) saturation indices (SI)s were determined for each sample by geochemical modeling in PHREEQC (Parkhurst and Appelo, 1999) using Aquachem version 3.742. Input parameters included cations, anions, alkalinity, and field chemistry obtained for each sample. PHREEQC uses the Davies equation to define activity coefficients, γ_i, of charged aqueous species:

$$\log \gamma_i = \frac{\sqrt{\mu}}{1 + \sqrt{\mu}} - 0.3\mu, \quad (6)$$

where μ is the ionic strength of the solution. Positive SI values indicate conditions supersaturated with respect to the mineral in question, whereas negative SI values indicate undersaturated conditions. SI values of zero denote samples at equilibrium with respect to the mineral, and indicate conditions where neither dissolution nor precipitation of minerals dominate the solution. Given uncertainties in analytical and thermodynamic data, SI values are accurate to ± 0.05, and values falling within the range of −0.05 to 0.05 are considered to be at equilibrium. Saturation indices were also determined for a theoretical mix that repeated in successive 5% increments between the freshest Keys' groundwater sample collected (well B26 in May 2011), hereafter referred to as fresh endmember, and the corresponding seawater sample obtained from the Gulf of Mexico for that time period (TBK in April 2011), hereafter referred to as ocean endmember. Modeling was done under closed-system conditions. The well selected as the freshwater endmember had salinities that varied little over the course of monthly sampling (0.3–0.6 ppt), with an average chloride concentration of 112 mg/L (minimum of 88 mg/L; maximum of 175 mg/L), falling far below the secondary standard for drinking water established by the EPA of 250 mg/L.

Percent of seawater comprising each groundwater and surface water sample was calculated from chloride concentrations (Cl^- in mmol/L) of each sample and the previously described endmembers using the following equation:

$$\frac{Cl^-_{sample} - Cl^-_{fresh\ endmember}}{Cl^-_{ocean\ endmember} - Cl^-_{fresh\ endmember}} * 100. \quad (7)$$

Average percent seawater composition over the course of the year sampling period was calculated for each site (well or surface water collection). Concentrations of calcium expressed in meq/L, were plotted against chloride in meq/L to determine if their concentrations could be explained by conservative mixing of fresh groundwater and seawater. Calcium excess, calculated as the difference between observed calcium and that predicted from conservative mixing, was compared to percent seawater for each groundwater sample for the months of May, August, November, and February. The chemical composition of each water sample was also plotted on a piper diagram. Seasonal changes in saturation indices and geochemistry were evaluated and compared to rainfall and PET over the study period.

2.6. Isotopic analysis

Following the procedure of Ellsworth and Sternberg (2015), groundwater, surface water, bay water, and rainfall samples were analyzed for stable isotopes of oxygen ($\delta^{18}O$) and hydrogen ($\delta\ ^2H$) on a GV IsoPrime™ isotope ratio mass spectrometer (IRMS) attached to a Multiflow system at the Laboratory of Stable Isotope Ecology in Tropical Ecosystems (LSIETE) at the University of Miami. Hydrogen isotope ratios of the water were obtained through a process of hydrogen equilibration with water vapor in the presence of platinum black powder (Prosser and Scrimgeour, 1995), while oxygen isotope ratios were obtained by equilibration with carbon dioxide (Vendramini and Sternberg, 2007). The results have a precision of ± 0.1‰ and ± 2.0‰ standard deviation for oxygen and hydrogen, respectively. Oxygen and hydrogen isotopic ratios for each sample were calculated according to the following equation:

$$\delta‰ = [(Rsample/R_{SMOW}) - 1] * 1000 \quad (8)$$

where R_{sample} and R_{SMOW} = $^{18}O/^{16}O$ or $^2H/H$ of the sample and standard mean ocean water (SMOW) (Craig, 1961). Groundwater $\delta^{18}O$ values and chloride composition of each water samples were compared (where data was available) to understand relative magnitude of evaporation effect across the seasons.

3. Results

3.1. Climate data

During the study period (April 2011 through March 2012) the lower Keys received 110.5 cm of rainfall, an amount slightly above the 30-year average for Key West of 102.7 + /2.8 − cm (1983–2012). However, for all months except July, October, and February, monthly rainfall was far below the 30-year monthly average for Key West (1983–2012) (Fig. 2), resulting in drought-like conditions for a large part of the wet-season that year. Over the course of a few days within the months of July and October, the lower Keys received half the rainfall for the entire study period, with 44 cm falling over 5 days in October. The total amount of precipitation received during October 2011 was more than three times the Key West 30-year average (13.9 ± 1.9 cm) for that month.

The relationship between precipitation and evapotranspiration over the study period was indicative of drought conditions punctuated by large rainfall events in July and October 2011 (Fig. 2). On average, the water balance of the wet season in south Florida (June through October) is positive, with precipitation greater than PET, while the dry season months display larger losses to potential evapotranspiration than the precipitation received (Abtew et al., 2011). However, during the study period, only in the months of July and October did precipitation totals surpass PET.

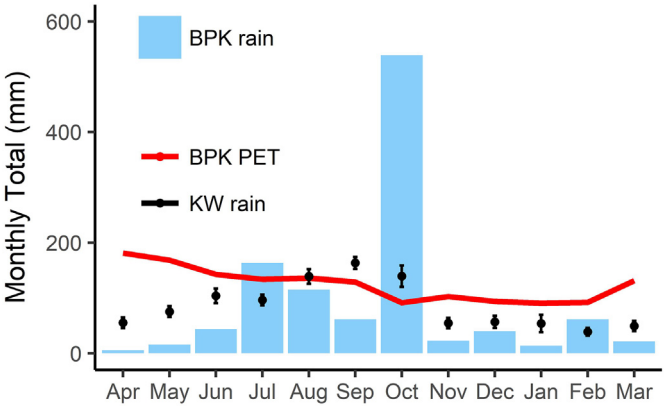

Fig. 2. Total monthly rainfall (mm) and potential evapotranspiration (PET) (mm) on Big Pine Key (BPK) from April 2011 through March 2012. Thirty-year average (1983–2012) monthly rain totals (mm) for Key West (KW) are included for comparison.

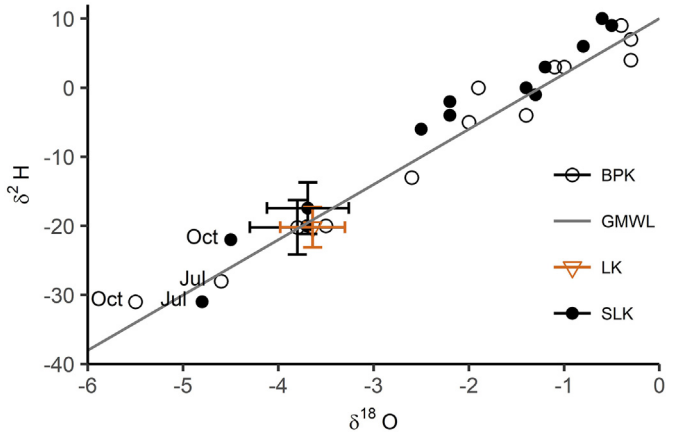

Fig. 3. Monthly $\delta^{18}O$ and $\delta^{2}H$ of rainwater on Big Pine Key (BPK) and Sugarloaf Key (SLK) from March 2011 through March 2012. Weighted-averages ± SE are denoted by error bars for BPK, SLK, and Long Key (LK) (from Price et al., 2008). Global mean water line (GMWL): $\delta^{2}H = \delta^{18}O*8 + 10‰$ (Craig, 1961). July and October 2011 rain labeled on graph.

3.2. Rainfall isotopes

The isotopic values for $\delta^{18}O$ and $\delta^{2}H$ obtained for the weighted-mean precipitation over the study period were − 3.80 ± 0.50‰ and − 20.2 ± 3.9‰ for BPK and − 3.69 ± 0.43‰ and − 17.43 ± 3.7‰ for SLK., All values corresponded closely to the previously reported values for precipitation collected on Long Key, located 65 km northeast of Big Pine (− 3.64 ± 0.34‰, − 20.2 ± 2.9‰) (Price et al., 2008) (Fig. 3). Values for each month fall along the Global Meteoric Water Line (GMWL) (Craig, 1961). The months of July and October 2011 have the most depleted values, consistent with rain derived from oceanic sources.

The average gulf water measured near Tarpon Belly Keys (1.54 ± 0.09‰ for $\delta^{18}O$, 8.3 ± 1.0‰ for $\delta^{2}H$, n = 4) agreed closely with previously reported values for sea water in Biscayne Bay near Elliott Key (1.7‰ for $\delta^{18}O$, 14‰ for $\delta^{2}H$) (Sternberg and Swart, 1987). As groundwater at each sampling site is a mixture of precipitation and seawater, its isotopic characteristics should fall between these two end-members at all sites (Fig. 4a, and b). Groundwater fell between the two end members of rain and gulf water, however most samples fell above the line, indicating the effect of evaporation on the shallow groundwater. After the large rain event in October, groundwater $\delta^{18}O$ signatures at several sampling locations fall below the conservative mixing line between the gulf water and average-weighted rain value, and instead approach a line between gulf water and the signature of October rain (Fig. 4b). These include groundwater sampling locations both at interior and exterior island locations that appear to be highly influenced by recharge events as they shifted by > 0.4 SE over the course of quarterly sampling.

3.3. Relationship between precipitation, salinity, and location on island

Results of monthly groundwater monitoring indicated that not only was groundwater salinity highest near the coast, but monthly changes were generally of larger magnitude at these coastal locations (Table 1, Fig. 5). Wells on SLK show a pattern of increasing variability around the mean salinity measurement along each transect from interior to coast that is not present on BPK (Table 1). Between sample events, decreasing groundwater salinity was observed following the two largest rain events of the study period (July 6th - 7th and October 15th - 19th). Half of the wells on SLK were highly responsive to freshwater input from the October rain event (Fig. 4b), while fewer sites on BPK exhibited the same decrease in $\delta^{18}O$ and groundwater salinity in response to precipitation. In fact, groundwater salinity in several wells on transects B1 and B3

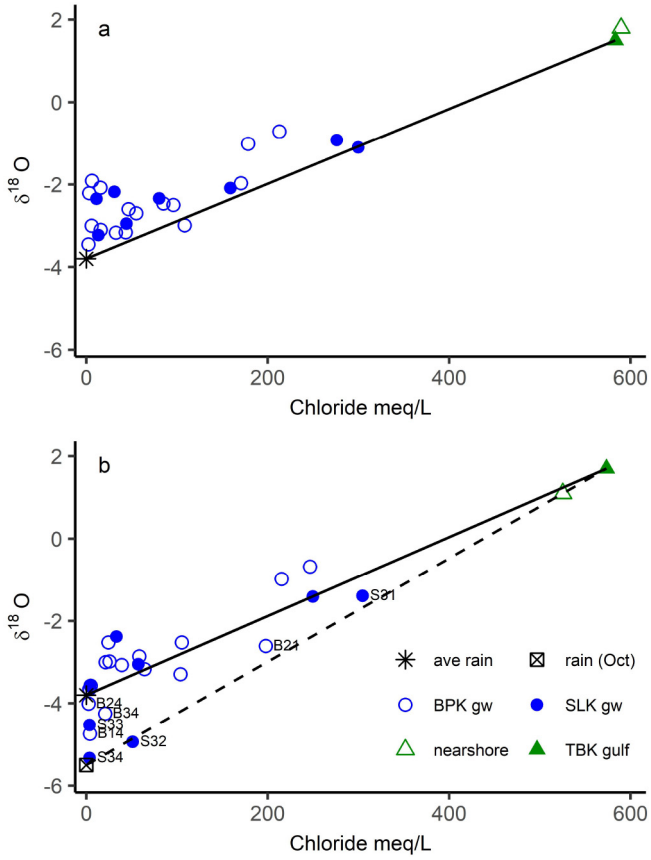

Fig. 4. Chloride in meq/L plotted against the $\delta^{18}O$ for groundwater samples (gw) collected from Big Pine Key (BPK) and Sugarloaf Key (SLK) in a) May 2011 and b) November 2011. The saltwater endmember used for the conservative mixing line (solid line) is the gulf water sample obtained at TBK in April and December 2011, respectively. The Big Pine Key weighted average for rainfall is displayed in both graphs, while the value for rain in the month of October 2011 is included in the November plot. The dashed line shows the conservative mixing line using October rain as the freshwater endmember. Groundwater samples having $\delta^{18}O$ SEs > 0.4 are labeled in figure b (n = 4).

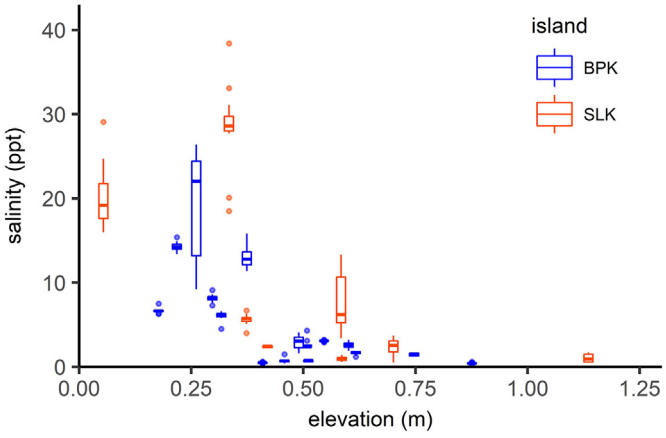

Fig. 5. Distribution of interquartile ranges (including outliers) of monthly groundwater salinity measurements (n = 12) for each site along the land-surface elevation gradient (m) for Big Pine Key (BPK) and Upper Sugarloaf Key (SLK).

actually increased after these rain events, perhaps as salts within the vadose zone were flushed into the aquifer. The average location of the water table below the ground surface was < 1 m for all wells (Table 1) and was positively correlated with the surface elevation as higher

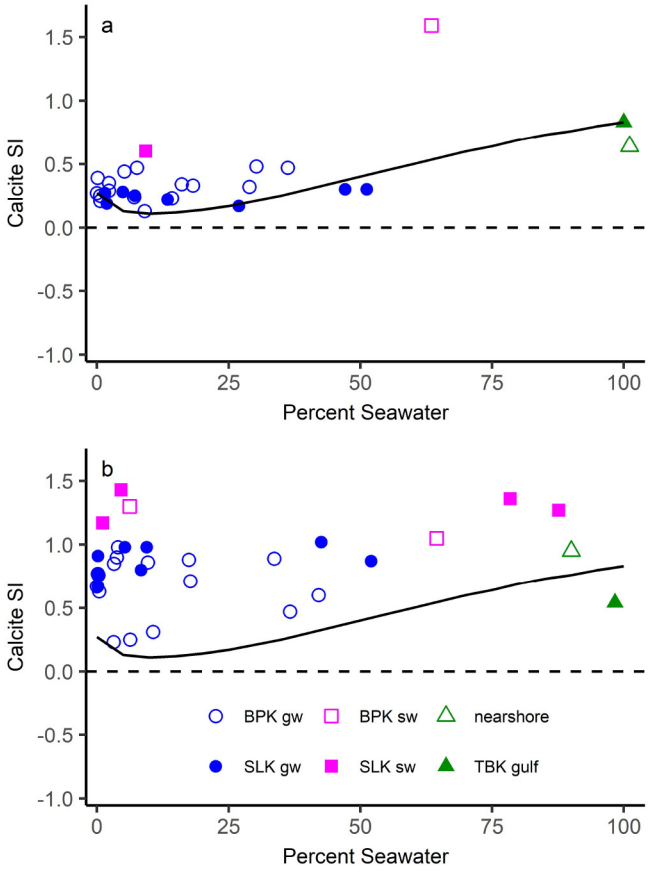

Fig. 6. Calcite saturation index (SI) of groundwater (gw) and surface water (sw) samples from Big Pine Key (BPK) and Upper Sugarloaf Key (SLK) compared to percent seawater of each sample for the months of a) May and b) November 2011. The solid line in both graphs represents the saturation state calculated by PHREEQC when mixing the freshest groundwater sample (B26 May 2011) with gulf water (TBK April) in closed-system conditions. The dashed line represents equilibrium conditions.

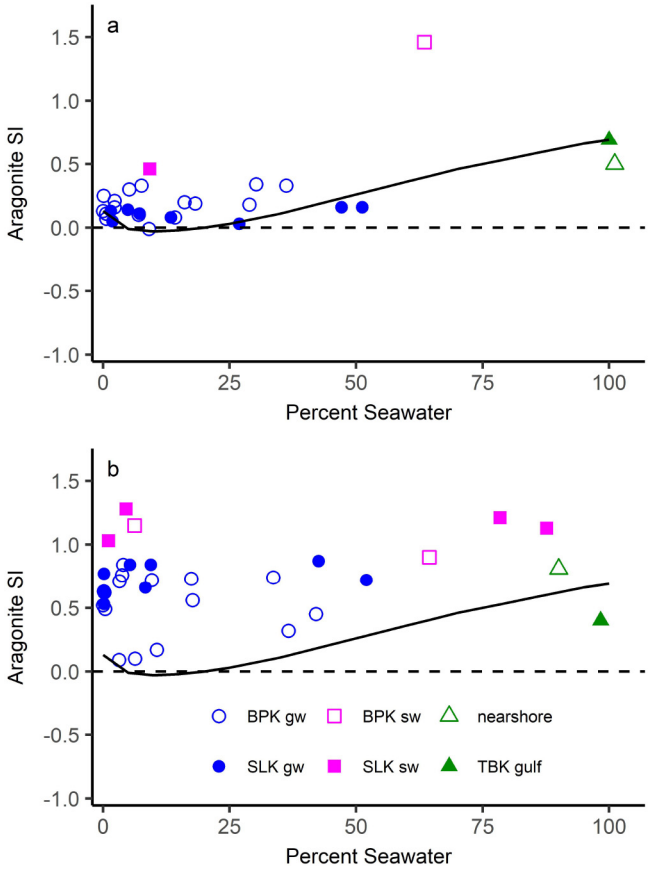

Fig. 7. Aragonite saturation index (SI) of groundwater (gw) and surface water (sw) samples from Big Pine Key (BPK) and Upper Sugarloaf Key (SLK) compared to percent seawater of each sample for the months of a) May and b) November 2011. The solid line in both graphs represents the saturation state calculated by PHREEQC when mixing the freshest groundwater sample (B26 may 2011) with gulf water (TBK April) in closed-system conditions. The dashed line represents equilibrium conditions.

elevation sites had larger unsaturated zones ($R^2 = 0.80$). The depth to the water table varied over the course of the study for each site by an average of 0.35 m, which is consistent with daily changes in tidal amplitude for Florida Bay in the vicinity of BPK and SLK.

3.4. Saturation indices and groundwater chemistry

The majority of groundwater samples were supersaturated with respect to calcite (Fig. 6) and aragonite (Fig. 7) in all months with some samples approaching equilibrium for calcite (SI = 0 ± 0.05) during the months of May through August, and October. Only two groundwater samples during the course of the study were slightly undersaturated with respect to aragonite - S32 in October (−0.12) and B24 in June (−0.06). Theoretical calculations between the freshest groundwater on the islands, obtained from well B26 in May, to that of corresponding gulf water sample predict that the saturation index of calcite would decrease to a minimum value of 0.11 at 10% seawater and increase to a maximum of 0.83. Similarly, equilibrium to slightly undersaturated conditions are predicted for aragonite at 10% sea water. Yet, samples do not vary with the percent seawater composition as predicted by the theoretical model. However, both SIs vary throughout the year for individual locations. The lowest SI values for most groundwater monitoring locations occurred in either July or October. Whereas the highest SIs were observed during November 2011, with the notable exception of the wells along transect B3 (Fig. 1), which had the highest SI values during the month of December 2011. The average monthly calcite SI for rainwater from FL11 was highly undersaturated at −6.98 ± 0.18 SE (n = 12).

Calcium (meq/L) was enriched relative to the seawater dilution line between the gulf sample and freshest groundwater sample for the majority of samples (Fig. 8). Exceptions included a few surface water samples which fell below the dilution line (Fig. 8b) and hypersaline surface water near the coast that fell along the dilution line (Fig. 8a). Locations of groundwater having the highest calcium concentrations occurred adjacent to the coast, with near-coast groundwater samples having the highest concentrations, some greater than the seawater endmember.

Calcium excess (meq/L), the amount of calcium in the sample greater than that predicted by conservative mixing between the freshest sample and gulf water, varied over the course of the study and along a gradient of increasing percent seawater of each sample (Fig. 9). A strong positive relationship (R^2 ranging from 0.46 to 0.82, $p < 0.01$) was observed on BPK between percent seawater and excess calcium, however, the relationships varied by month, as did the amounts observed at each site. On SLK, a weaker relationship was observed between calcium excess and percent seawater, with only February significant at $p < 0.01$ (Fig. 9). The slope of the relationship between percent seawater and calcium excess was steeper on BPK, about 5 times that of SLK, having an average increase of 0.2 in excess calcium for each 1% increase in percent seawater (Fig. 9). By site, the greatest calcium excess was generally observed in November for BPK, whereas SLK had the largest amounts in May and August.

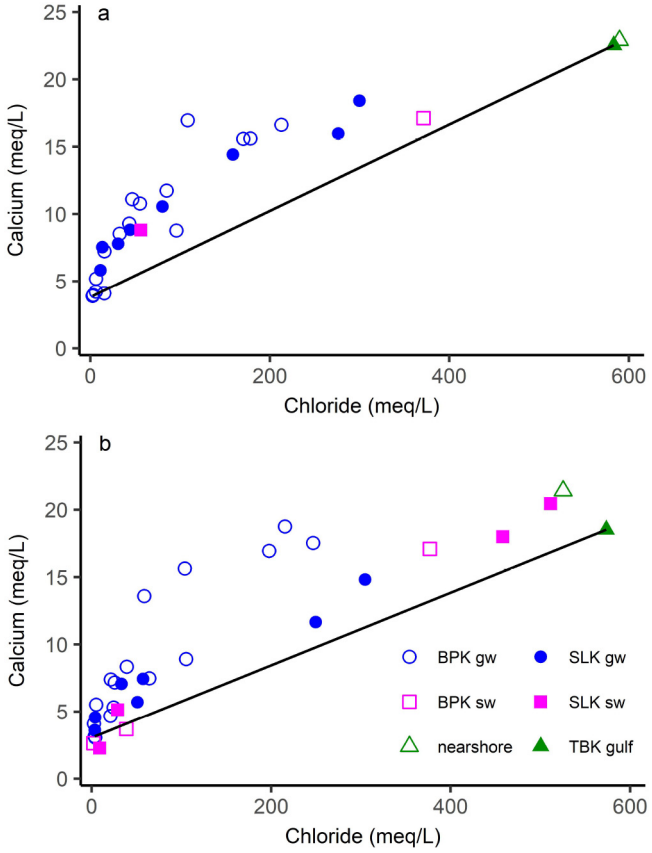

Fig. 8. The amount of calcium (meq/L) compared to chloride (meq/L) in (gw) and surface water (sw) samples from Big Pine Key (BPK) and Upper Sugarloaf Key (SLK) for the months of a) May and b) November 2011. The endpoints of the conservative mixing line (solid line) include the groundwater sample with the lowest conductivity and the corresponding gulf water sample (TBK) of the month represented.

Composition of groundwater was plotted on a piper diagram for all wells for each transect. Samples generally varied from Ca-HCO_3 type waters to Na-Cl type waters, with two-thirds of wells described as having solely Na-Cl type waters. Transect S3 (Fig. 10) on SLK is of particular interest as groundwater samples obtained from wells S33 – S35 did not cluster in a single location, but instead varied throughout the study. The composition of S33 and S34 changed from a Na-Cl to a Ca-Na-HCO_3 type water after the October rain event. The groundwater sample having the largest range in composition was S33, which traverses the piper diagram along the Cl axis, whereas S34 clusters in two distinct groups, pre- and post-October rain event.

4. Discussion

The balance between precipitation and evapotranspiration in the Florida Keys typically results in conditions of water deficit throughout the year. This was magnified during the study period (2011 – 2012) as the dry season extended well into the typical wet season and was finally broken by high-intensity rainfall events. Evaporative conditions are common in the Florida Keys and Florida Bay (Price et al., 2007). Shallow groundwater can also experience evaporation (Johnson et al., 2010). The enriched values of $\delta^{18}O$ of the groundwater (compared to what would be predicted from conservative mixing of rainwater and gulf endmember) can be a result of direct evaporation of the groundwater, or infiltration of surface water exposed to evaporation (Price and Swart, 2006). Large rainfall events with depleted $\delta^{18}O$ values, compared to the weighted-average rainfall, are useful in determining spatial and temporal changes in the aquifer as several locations on both SLK and BPK had $\delta^{18}O$ values of groundwater highly influenced by recent rain (Fig. 4b). This was readily observed along the S3 transect on SLK, and suggests a single large rainfall event can play a critical role in aquifer recharge of a small island (Fig. 10).

The results of theoretical mixing of freshwater and seawater for both calcite and aragonite saturation indices indicate a narrow range of salinities where conditions were favorable for carbonate mineral dissolution. In all months, the overwhelming majority of groundwater samples were supersaturated with respect to both aragonite and calcite, and only approached equilibrium conditions in the height of the dry season, most likely in response to precipitation of calcium carbonate minerals. Contrary to expectations and processes observed on other limestone platforms (Back et al., 1986; Mylroie and Carew, 1990) our results suggest that dissolution of the limestone bedrock within the brackish groundwater mixing zone is not expected within the first meter of the saturated zone of the aquifers on either BPK or SLK. A lack of undersaturated conditions within the mixing zone of other carbonate islands has been observed and attributed to a variety of conditions including CO_2 degassing (Plummer et al., 1976, Price and Herman, 1991; Gulley et al., 2015, 2016). Degassing of CO_2 likely plays a large role in the supersaturated conditions observed at our sites. Although we do not believe any substantial degassing occurred during sample collection, the potential for CO_2 outgassing during the measurement of pH was possible and could have a substantial influence on the determination of the saturation indices (Pearson Jr. et al., 1978). Furthermore, the highly karsified surficial bedrock allows for numerous direct pathways for CO_2 to degas from the shallow water table to the atmosphere. Additionally, tidal pumping within the lens, even a microtidal range of 0.3 as is observed in the lower Florida Keys, could increase dispersive transport of CO_2 and additional degassing (Hanor, 1978).

Much of the excess calcium observed in the groundwater samples is likely derived from dissolution of the limestone bedrock in the vadose zone upon contact with highly undersaturated rainwater and subsequent transport to the groundwater upon infiltration. Calcite is reported to be the dominant mineral in the Biscayne Aquifer limestone, with only minor amounts of aragonite (Evans and Ginsburg, 1987), so there is some potential for the observed excess calcium to be in response to the common ion effect, as aragonite solubility is higher than calcite. The high calcium excess observed in the groundwater samples in November on BPK, following a high intensity rainfall event in October (Fig. 7b) supports the conclusion that most of the excess calcium is from limestone dissolution in the vadose zone as opposed to mixing of fresh groundwater and seawater.

The varying R^2 and slope of the relationship of calcium excess with percent seawater between the two islands points to different processes that potentially dominate as a function of island size and topography (Fig. 9). The higher elevations and larger amount of land area above mean sea level (amsl) on BPK result in a larger vadose zone in which a greater quantity of limestone dissolution can take place with subsequent transport of Ca^{2+} ions to the groundwater table and ultimately to the coastline with groundwater discharge. In contrast, the lower R^2 and rather flat slope between calcium excess with percent seawater in the groundwater of SLK may be attributable to its smaller size and lower topography limiting the extent of the vadose zone available for carbonate mineral dissolution.

Besides freshwater-seawater mixing, other researchers have suggested alternative processes are important in determining the geochemistry of carbonate islands. For instance, Gulley et al. (2016) have identified heterogenous increases in pCO_2 as driving limestone dissolution leading to cave formation. Increases in pCO_2 could result from the remineralization of organic matter from the soil and movement of dissolved organic carbon across the thin vadose zone (Gulley et al., 2015). Vertical conduits through the vadose zone can also be avenues for rapid transit of organic carbon to the water table leading to heterogeneous zones of pCO_2 (Gulley et al., 2015). Both BPK and SLK contain upland pine and hardwood forests and coastal mangroves

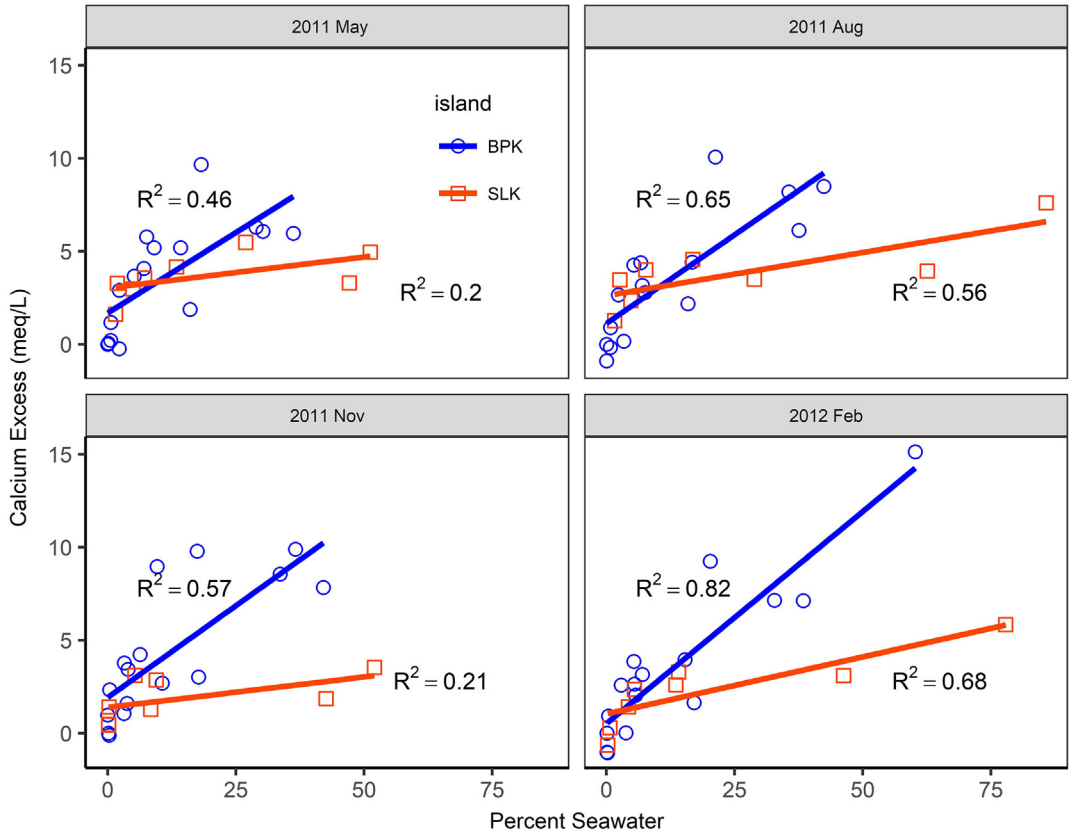

Fig. 9. Calcium excess in meq/L plotted against percent seawater of each groundwater sample for Big Pine Key (BPK) and Upper Sugarloaf Key (SLK) for the months of May, August, November, and February.

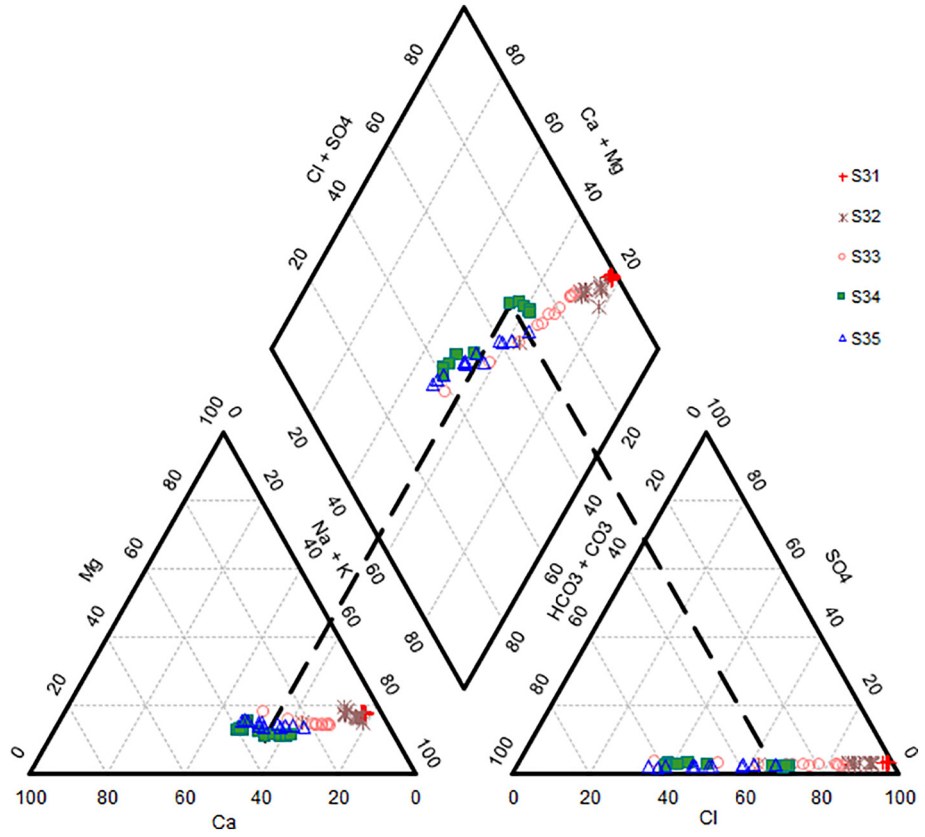

Fig. 10. Piper diagram of major cations and anions for groundwater samples from wells S31 through S35 (Transect S3) on SLK. The dashed line points to the position of S34 well samples in the diagram during the months of May through October 2011.

overlying karst bedrock. Groundwater on these islands could experience changing pCO_2 conditions as it flows from the interior to edge of the islands, as pine forests, subtropical hardwoods, and mangroves may vary in their CO_2 production as well as their contributions of organic matter in the subsurface. Higher amounts of excess calcium were generally observed on SLK in May and August as opposed to November, coinciding with peaks in soil respiration observed for other subtropical forests (Tan et al., 2013). Perhaps increased pCO_2 from soil respiration plays an increasingly important role in limestone dissolution as the area for interaction with meteoric waters shrinks on a small island like SLK. Further research is required to determine the relationships between forest type, plant growth, CO_2 production and limestone dissolution on both BPK and SLK.

The sustained supersaturated conditions with respect to the carbonate minerals in the higher salinity groundwaters in both BPK and SLK suggest the potential for carbonate mineral precipitation and not dissolution along the islands edge. Subsequent evaporation of both groundwater and overland flow results in carbonate deposition forming a hard cement or “case hardening” (Ford and Williams, 2007) of the surface bedrock. Hard rock conditions were observed at both BPK and SLK sites located in depressions and adjacent to the mangrove shoreline as those wells were typically difficult to drill. The cementation produced a relatively flat bedrock surface at those locations. Tidal inundation in the most shoreward sites also resulted in standing water and subsequent evaporation leading to hypersaline conditions (surface water sites, Table 1) which can also lead to deposition of evaporite minerals including carbonates. Hypersaline conditions leading to formation of evaporite minerals have been observed in the interior of small mangrove islands in Florida Bay (Juster et al., 1997) as well as in the Yucatan Peninsula (Perry et al., 2003).

The wide variation in groundwater composition throughout the study of wells on SLK, specifically wells S33, S34, and S35, (Fig. 10) indicates rapidly changing groundwater conditions in response to the climate variables of rainfall and ET. Of the five transects crossing the gradient of upland to coast, the northern transect on SLK was the only place we observed this phenomenon. The S34 well, located at the highest elevation on the island, was primarily influenced by Ca-HCO_3 waters until the conclusion of the study, more than five months after the rain event in October 2011. The impact of the rainfall event was shorter-lived at S33, located 50 m coastward of S34, having a post-rainfall groundwater composition similar to that of the S34 and S35 wells until January 2012. The change in the S33 well from brackish (well S32) to fresh (well S34) composition provides an indicator of the potential increase in the size of the freshwater lens on SLK between dry and wet season conditions. Using the boundary of the freshwater lens on SLK as derived by Meadows et al. (2004), we estimate a maximum aerial extent in the form of an ellipse, with semi-major axis of 600 m and semi-minor axis of 200 m, equal to 0.38 km^2. As the groundwater composition of S33 moves to that of S34, we can use the horizontal distance between these adjacent wells as the distance of boundary fluctuation. If we assume this happens on all sides of the ellipse, both axes decrease by 50 m, resulting in a dry season lens equal to 0.26 km^2. This equates to a 45% increase in lens extent from dry to wet seasons.

The seasonal change from a Na-Cl type water in the dry season to a Ca-Na-HCO_3 in the wet season is a strong indication that the lens on SLK is relatively unstable compared to that of BPK, with implications for both the supply of freshwater and groundwater geochemistry. This difference in groundwater geochemistry between the islands could be explained by the size of the freshwater lens on each island: the northern lens of BPK is more than an order of magnitude larger than that of SLK (Wightman, 1990; Meadows et al., 2004),. The seasonal change in groundwater composition on SLK is additionally supported by results of electrical resistivity tomography surveys conducted in May and November 2011 along the S2 and S3 transects that show lateral movement of the lens boundary with wet season precipitation (Ogurcak, 2015). These results suggest that the freshwater lens found on smaller carbonate islands, such as SLK, are more susceptible to perturbations related to rainfall events, seasonal fluctuations in ET and tidal pumping.

4.1. The impacts of future climate change and sea level rise

Impacts of a warming climate and accelerated sea level rise will disproportionally impact aquifers on low-elevation islands and coastal zones, especially in places heavily reliant on recharge from rain. Coastlines dominated by carbonates could face additional challenges as a function of their close relationship with the sea. Increased air temperatures will result in enhanced evapotranspiration in shallow aquifers. Combined with the predicted summer drying trend in the Caribbean region (Neelin et al., 2006), freshwater lenses in the lower Florida Keys and the greater Caribbean region, including the Bahamas and the Yucatan, will shrink and become increasingly intruded by saline water. Higher sea surface temperatures will lead to increased number of extreme rainfall events, and reliance of aquifers on recharge from such events as observed in the Keys in October of 2011 may become the norm. Increasing rates of sea level rise will disproportionally impact small islands like those of the Florida Keys, as the extent of freshwater lenses shrink with island area.

The comparison between two islands of similar geology but varying size allow us to substitute space for time with the current conditions observed in the fresh water lens on SLK might be expected on BPK in the next century, given sea level rise projections (Church et al., 2013). The small freshwater lens observed on SLK is more susceptible to changing geochemical conditions in response to high rainfall events, ET and saltwater intrusion (Fig. 10). Higher sea levels will not only result in decreasing the horizontal extent of the freshwater lens on island, but will also raise the less dense freshwater lens upward reducing the vertical thickness of the vadose zone (Saha et al., 2011). A thinner vadose zone diminishes the amount of limestone susceptible to dissolution by meteoric waters as suggested by the smaller calcium excess observed on SLK (Fig. 9). A shallow water table can lead to enhanced surface water ponding during high rain events as the thin vadose zone will quickly fill with freshwater. Initially the rain and ponded surface water will dissolve limestone at or near the surface. Subsequent exposure to evaporation will result in precipitation of carbonates in place and the creation of a limestone pavement decreasing the island's infiltration capacity. Future large rain events would be expected to result in higher overland flow and less aquifer recharge.

5. Conclusion

We studied the chemical composition of groundwater on two small carbonate islands in the Florida Keys, BPK and SLK. We found that although the groundwater chemistry on both islands was susceptible to changes in rainfall, ET and sea level rise, groundwater conditions on the smaller island (SLK) were more variable. During most of the study period, ET exceeded rainfall allowing saltwater to intrude along the edges of the islands reducing the size of the fresh water lens, with a smaller freshwater lens observed on the smaller island (SLK). A large rainfall event in October 2011 was successful in recharging the aquifers on both islands as indicated by oxygen isotopes, and by changing the groundwater chemistry in portions of the smaller island from a Na-Cl type water to a Ca-HCO_3 type water. We did not find evidence of mixing zone groundwater undersaturated with respect to the carbonate minerals on either island, instead supersaturated conditions prevailed in all groundwater samples. Excess calcium compared to conservative mixing with fresh groundwater and seawater was observed in most groundwater samples, with a higher calcium excess observed on the larger island (BPK). We postulated that the excess calcium derived from limestone dissolution in the vadose zone upon contact with highly undersaturated rainwater and transported to the groundwater through infiltration. The larger island (BPK) had a higher calcium excess probably in response to a larger vadose zone. Degassing of CO_2 from the

groundwater table could be responsible for the sustained supersaturated conditions with respect to the carbonate minerals. Carbonate mineral precipitation is expected from the brackish groundwaters along the island's edge, as well as at the surface in response to evaporation of surface water. Sea level rise is expected to decrease the size of both the freshwater lens and the vadose zone on small carbonate islands, reducing the potential for limestone dissolution.

Acknowledgments

We thank Anne Morkill and Phillip Hughes at the National Key Deer Refuge for logistical support and John DeMott for access to his property. Many thanks to Pablo Ruiz, Diane Pirie, Pamela Sullivan, David Lagomasino and numerous other individuals that assisted with installation of the groundwater monitoring network. Thank you to Jonathan Martin and an anonymous reviewer for helpful comments on the manuscript. This work was supported by the U.S. Department of the Interior Fish and Wildlife Service, USA under contract number F12AC01508. Danielle Ogurcak was supported by the Florida International University Doctoral Evidence Acquisition Fellowship. This is contribution number 890 from the Southeast Environmental Research Center in the Institute of Water & Environment at Florida International University.

References

Abtew, W., 1996. Evapotranspiration measurements and modeling for three wetland systems in South Florida. J. Am. Water Resour. Assoc. 32, 465–473. https://doi.org/10.1111/j.1752-1688.1996.tb04044.x.

Abtew, W., Obeysekera, J., Iricanin, N., 2011. Pan evaporation and potential evaporation trends in South Florida. Hydrol. Process. 25, 958–969.

Anthony, S.S., Peterson, F.L., MacKenzie, F.T., Hamlin, S.N., 1989. Geohydrology of the Laura fresh-water lens, Majuro atoll: a hydrogeochemical approach. Geol. Soc. Am. Bull. 101, 1066–1075.

Back, W., Hanshaw, B.B., 1970. Comparison of chemical hydrogeology of the carbonate peninsulas of Florida and Yucatan. J. Hydrol. 10, 330–368. https://doi.org/10.1016/0022-1694(70)90222-2.

Back, W., Hanshaw, B.B., Herman, J.S., Van Driel, J.N., 1986. Differential dissolution of a Pleistocene reef in the ground-water mixing zone of coastal Yucatan, Mexico. Geology 14, 137–140.

Childers, D.L., Boyer, J.N., Davis, S.E., Madden, C.J., Rudnick, D.T., Sklar, F.H., 2006. Relating precipitation and water management to nutrient concentrations in the oligotrophic “upside-down” estuaries of the Florida Everglades. Limnol. Oceanogr. 51, 602–616.

Church, J.A., Clark, P.U., Cazenave, A., Gregory, J.M., Jevrejeva, S., Levermann, A., Merrifield, M.A., Milne, G.A., Nerem, R.S., Nunn, P.D., Payne, A.J., Pfeffer, W.T., Stammer, D., Unnikrishnan, A.S., 2013. Sea level change. In: Stocker, T.F., Qin, D., Plattner, G.-K., Tignor, M., Allen, S.K., Boschung, J., Nauels, A., Xia, Y., Bex, V., Midgley, P.M. (Eds.), Climate Change 2013: The Physical Science Basis. Contribution of Working Group I to the Fifth Assessment Report of the Intergovernmental Panel on Climate Change. Cambridge University Press, Cambridge, United Kingdom and New York, NY, USA.

Coniglio, M., Harrison, R.S., 1983. Facies and diagenesis of late Pleistocene carbonates from Big Pine Key, FL. Bull. Can. Petrol. Geol. 31, 135–147.

Craig, H., 1961. Standard for Reporting Concentrations of Deuterium and Oxygen-18 in Natural Waters. Science 133, 1833–1834. https://doi.org/10.1126/science.133.3467.1833.

DiFrenna, V.J., Price, R.M., Savabi, M.R., 2008. Identification of a hydrodynamic threshold in karst rocks from the Biscayne Aquifer, South Florida, USA. Hydrogeol. J. 16, 31–42. https://doi.org/10.1007/s10040-007-0219-4.

Duever, M.J., Meeder, J.F., Meeder, L.C., McCollom, J.M., 1994. The climate of south Florida and its role in shaping the Everglades ecosystem. In: Davis, S.M., Ogden, J.C. (Eds.), Everglades: The Ecosystem and its Restoration. St. Lucie Press, pp. 225–248.

Ellsworth, P.Z., Sternberg, L.S.L., 2015. Seasonal water use by deciduous and evergreen woody species in a scrub community is based on water availability and root distribution. Ecohydrology 8, 538–551. https://doi.org/10.1002/eco.1523.

Evans, C.C., Ginsburg, R.N., 1987. Fabric selective diagenesis in the late Pleistocene Miami Limestone. J. Sediment. Petrol. 41, 311–318.

Flower, H., Rains, M., Lewis, D., Zhang, J.-Z., Price, R., 2017. Saltwater intrusion as potential driver of phosphorus release from limestone bedrock in a coastal aquifer. Estuar. Coast. Shelf Sci. 184, 166–176. https://doi.org/10.1016/j.ecss.2016.11.013.

Ford, D., Williams, P.D., 2007. Karst hydrogeology and geomorphology. Wiley, England (576pp).

Gulley, J.D., Martin, J.B., Moore, P.J., Brown, A., Spellman, P.D., Ezell, J., 2015. Heterogeneous distributions of CO_2 may be more important for dissolution and karstification in coastal eogenetic limestone than mixing dissolution. Earth Surf. Process. Landf. 40 (8), 1057–1071.

Gulley, J.D., Martin, J.B., Brown, A., 2016. Organic carbon inputs, common ions, and degassing: rethinking mixing dissolution in coastal eogenetic carbonate aquifers. Earth Surf. Process. Landf. 41, 2098–2110.

Hanor, J.S., 1978. Precipitation of beachrock cements: mixing of marine and meteoric waters vs. CO2-degassing. J. Sediment. Res. 48.

Hanson, C.E., 1980. Freshwater Resources of Big Pine Key, FL (No. OF 80-447). U.S. Department of the Interior Geologic Survey, Tallahassee, FL.

Harrison, R.S., Coniglio, M., 1985. Origin of the Key Largo Limestone, Florida Keys. Bull. Can. Petrol. Geol. 33, 350–358.

Hoffmeister, J.E., Multer, H.G., 1968. Geology and origin of the Florida Keys. Geol. Soc. Am. Bull. 79, 1487–1502.

Hoffmeister, J.E., Stockman, K.W., Multer, H.G., 1967. Miami Limestone of Florida and its recent Bahamian counterpart. Geol. Soc. Am. Bull. 78, 175–190.

Johnson, E., Yáñez, J., Ortiz, C., Muñoz, J., 2010. Evaporation from shallow groundwater in closed basins in the Chilean Altiplano. Hydrol. Sci. J. 55, 624–635. https://doi.org/10.1080/02626661003780458.

Juster, T., Kramer, P.L., Vacher, H.L., Swart, P.K., 1997. Groundwater flow beneath hypersaline pond, Cluett Key, Florida Bay, FL. J. Hydrol. 197, 339–369.

Keim, B.D., Muller, R.A., Stone, G.W., 2007. Spatiotemporal patterns and return periods of tropical storm and hurricane strikes from Texas to Maine. J. Clim. 20, 3498–3509. https://doi.org/10.1175/JCLI4187.1.

Kulshrestha, U.C., Granat, L., Rodhe, H., 2003. Precipitation chemistry studies in India—a search for regional patterns. In: Report CM-99 Department of Meteorology. Stockholm University.

Langevin, C.D., Stewart, M.T., Beaudoin, C.M., 1998. Effects of sea water canals on freshwater resources: an example from Big Pine Key, FL. Groundwater 36, 503–513.

Langmuir, D., 1997. Aqueous Environmental Geochemistry. Prentice-Hall, Upper Saddle River, NJ.

Lee, K., Tong, L.T., Millero, F.J., Sabine, C.L., Dickson, A.G., Goyet, C., Park, G., Wanninkhof, R., Feely, R.A., Key, R.M., 2006. Global relationships of total alkalinity with salinity and temperature in surface waters of the world's oceans. Geophys. Res. Lett. 33, L19605. https://doi.org/10.1029/2006GL027207.

Meadows, D.G., Caballero, J.P., Kruse, S.E., Vacher, H.L., 2004. Variation of salinity in brackish-water lenses of two Florida Keys. J. Coast. Res. 20, 386–400.

Mylroie, J.E., Carew, J.L., 1990. The flank margin model for dissolution cave development in carbonate platforms. Earth Surf. Process. Landf. 15, 413–424.

Neelin, J.D., Münnich, M., Su, H., Meyerson, J.E., Holloway, C.E., 2006. Tropical drying trends in global warming models and observations. Proc. Natl. Acad. Sci. 103, 6110–6115.

Obeysekera, J., Barnes, J., Nungesser, M., 2015. Climate sensitivity runs and regional hydrologic modeling for predicting the response of the greater Florida Everglades ecosystem to climate change. Environ. Manag. 55, 749–762. https://doi.org/10.1007/s00267-014-0315-x.

Ogurcak, D.E., 2015. The Effect of Disturbance and Freshwater Availability on Lower Florida Keys' Coastal Forest Dynamics (Ph.D. Thesis). Florida International University, Miami, FL.

Parkhurst, D.L., Appelo, C.A.J., 1999. User's guide to PHREEQC (version 2) - a computer program for speciation, batch-reaction, one-dimensional transport, and inverse geochemical calculations. In: U.S. Geological Survey Water-Resources Investigations Report 99-4259, (312 p).

Pearson Jr., F.J., Fisher, D.W., Plummer, L.N., 1978. Correction of ground-water chemistry and carbon isotopic composition for effects of CO_2 outgassing. Geochim. Cosmochim. Acta 42 (12), 1799–1807.

Perkins, R.D., 1977. Depositional framework of pleistocene rocks in south Florida. In: Enos, P., Perkins, R.D. (Eds.), Quarternary Sedimentation in South Florida. Geological Society of America, pp. 131–198.

Perry, E., Velazquez-Oliman, G., Socki, R.A., 2003. Hydrogeology of the Yucatan Peninsula. In: Gomez-Pompa, A., Allen, M.F., Fedick, S.L., Jimenez-Osornio, J.J. (Eds.), The Lowland Maya Area: Three Millennia at the Human-Wildland Interface. Food Products Press, pp. 115–138.

Plummer, L.N., Vacher, H.L., Mackenzie, F.T., Bricker, O.P., Land, L.S., 1976. Hydrogeochemistry of Bermuda: a case history of ground-water diagenesis of bio-calcarenites. Geol. Soc. Am. Bull. 87, 1301–1316.

Price, R.M., Herman, J.S., 1991. Geochemical investigation of salt-water intrusion into a coastal carbonate aquifer: Mallorca, Spain. Geol. Soc. Am. Bull. 103, 1270–1279.

Price, R.M., Swart, P.K., 2006. Geochemical indicators of groundwater recharge in the surficial aquifer system, Everglades National Park, Florida, USA. In: Harmon, R.S., Wicks, C. (Eds.), Perspectives on Karst Geomorphology, Hydrology, and Geochemistry, pp. 251–266.

Price, R.M., Nuttle, W.K., Cosby, B.J., Swart, P.K., 2007. Variation and uncertainty in evaporation from a subtropical estuary: Florida Bay. Estuar. Coasts 30, 497–506.

Price, R.M., Swart, P.K., Willoughby, H.E., 2008. Seasonal and spatial variation in the stable isotopic composition (δ18O and δD) of precipitation in South Florida. J. Hydrol. 358, 193–205. https://doi.org/10.1016/j.jhydrol.2008.06.003.

Price, R.M., Savabi, M.R., Jolicoeur, J.L., Roy, S., 2010. Adsorption and desorption of phosphate on limestone in experiments simulating seawater intrusion. Appl. Geochem. 25, 1085–1091. https://doi.org/10.1016/j.apgeochem.2010.04.013.

Prosser, S.J., Scrimgeour, C.M., 1995. High-precision determination of 2H/1H in H2 and H2O by continuous-flow isotope radio mass spectrometry. Anal. Chem. 67, 1992–1997.

Robinson, R.B., 1967. Diagnesis and porosity development in recent and Pleistocene oolites from southern Florida and the Bahamas. J. Sediment. Petrol. 37, 355–364.

Ross, M.S., O'Brien, J.J., da Silveira Lobo Sternberg, L., 1994. Sealevel rise and the reduction in pine forests in the Florida keys. Ecol. Appl. 4, 144–156.

Saha, A.K., Saha, S., Sadle, J., Jiang, J., Ross, M.S., Price, R.M., Sternberg, L.S., Wendelberger, K.S., 2011. Sea level rise and South Florida coastal forests. Clim. Chang. 107, 81–108.

Scholl, M.A., Ingebritsen, S.E., Janik, C.J., Kauahikaua, J.P., 1996. Use of precipitation and ground water isotopes to interpret regional hydrology on a tropical volcanic island: Kileauea volcano area, Hawaii. Water Resour. Res. 32, 3525–3537.
Sternberg, L.S.L., Swart, P.K., 1987. Utilization of freshwater and ocean water by coastal plants of southern Florida. Ecology 68, 1898–1905.
Swart, P.K., Kramer, P.A., 1997. Geology of mud islands in Florida Bay. In: Vacher, H.L., Quinn, T.M. (Eds.), Geology and Hydrogeology of Carbonate Islands, Developments in Sedimentology. Elsevier Science, Netherlands, pp. 249–274.
Tan, Z., Zhang, Y., Liang, N., Song, Q., Liu, Y., You, G., Li, L., Wu, C., Lu, Z., Wen, H., Zhao, J., Gao, F., Yang, L., Song, L., Zhang, Y., Munemasa, T., Sha, L., 2013. Soil respiration in an old-growth subtropical forest: patterns, components, and controls. J. Geophys. Res. Atmos. 118, 2981–2990.
Vacher, H.L., Wightman, M.J., Stewart, M.T., Fletcher III, C.H., Wehmiller, J.F., 1992. Hydrology of meteoric diagenesis: effect of Pleistocene stratigraphy on freshwater lenses of Big Pine Key, Florida. In: Quarternary Coasts of the United States: Marine and Lacustine Systems. SEPM (Society for Sedimentary Geology), pp. 213–219.
Vendramini, P.F., Sternberg, L.S.L., 2007. A faster plant stem-water extraction method. Rapid Commun. Mass Spectrom. 21, 164–168.
Wightman, M.J., 1990. Geophysical Analysis and Dupuit-Ghyben-Herzberg Modeling of Freshwater Lenses on Big Pine Key, Florida (M.S. Thesis). University of South Florida, Tampa, FL.
Wong, P.P., Losada, I.J., Gattuso, J.-P., Hinkel, J., Khattabi, A., McInnes, K.L., Saito, Y., Sallenger, A., 2014. Coastal systems and low-lying areas. In: Field, C.B., Barros, V.R., Dokken, D.J., Mach, K.J., Mastrandrea, M.D., Bilir, T.E., Chatterjee, M., Ebi, K.L., Estrada, Y.O., Genova, R.C., Girma, B., Kissel, E.S., Levy, A.N., MacCracken, S., Mastrandrea, P.R., White, L.L. (Eds.), Climate Change 2014: Impacts, Adaptation, and Vulnerability. Part A:Global and Sectoral Aspects. Contribution of Working Group II to the Fifth Assessment Report of the Intergovernmental Panel on Climate Change. Cambridge University Press, Cambridge, United Kingdom and New York, NY, USA, pp. 361-40.
Zhang, K., Ross, M.S., Ogurcak, D.E., Houle, P., 2010. Lower Florida Keys digital terrain model and vegetation analysis for the National Key Deer Refuge (Final Report submitted to the U.S. Fish and Wildlife Service National Key Deer Refuge, Big Pine Key, FL). Florida International University, Miami, FL.